REACTION KINETICS OF METHANE COMBUSTION OVER $La_{1-x}Ca_xFeO_3$ PEROVSKITES

GINA PECCHI, M. GRACIELA JILIBERTO, EDUARDO J. DELGADO*

Department of Physical-Chemistry, Facultad de Ciencias Químicas, Casilla 160-C, Universidad de Concepción, Concepción, Chile.
(Received: March 15, 2011 - Accepted: September 8, 2011)

ABSTRACT

The reaction kinetics of methane combustion over $La_{1-x}Ca_xFeO_3$ perovskites (x=0.0, 0.2, 0.4) was studied. The results show that the catalytic activity is higher in the calcium-doped perovskites. It is found that this higher catalytic activity is related to a lower activation energy. The value of the activation energy is not affected by the level of Ca-doping. The observed difference in the catalytic activity between the doped perovskites is interpreted as a consequence of the so-called compensatory effect, i.e., a larger pre-exponential factor which results from the higher number of active sites promoted by defect reactions triggered by the substitution of lanthanum by calcium. The substitution of lanthanum by a lower valence cation, as calcium, entails both the formation of oxygen vacancies and oxidation of some iron ions from Fe^{3+} to Fe^{4+}, in order to preserve the electroneutrality. The oxygen vacancies account for the increasing participation of lattice oxygen in the combustion kinetics as the calcium doping increases. The experimental results were satisfactorily fitted to the Rideal-Elay mechanism.

Keywords: methane, combustion, perovskite, defects, kinetic

INTRODUCTION

The global pollution by harmful species such as CO and NO_x has motivated legislative restrictions more and more demanding for gaseous emissions from either fossil fuel burners or vehicles. This scenario has stimulated the research on novel catalysts for combustion of hydrocarbons. In this context, catalytic combustion represents an attractive alternative compared to conventional flame combustion. Among the advantages are a wide range of concentrations of hydrocarbons and the possibility to operate outside the flammability limits of fuels. Traditional catalysts for methane combustion are supported noble metals. These materials show high activity even at low temperature, but their commercial use is limited by reasons of high volatility of oxides, sintering and mainly by cost. Therefore, there has been much interest in the development of catalysts based on mixtures of selected metal oxides instead of noble metals. Perovskite-like mixed oxides, with general formula ABO_3, showed suitable catalysts for oxidation of light hydrocarbons and, in particular, of methane [1-6].

Perovskites can be tailored to create a wide family of catalysts, by varying either the A-site or the B-site metal ion, or both. Indeed, the catalytic activity of a perovskite can be modified by inserting proper transition metal ions. Partial substitution at the A-site with another metal cation, doping, can strongly affect the catalytic activity due to stabilisation of unusual oxidation states of the B cation and simultaneous formation of structural defects created by such a substitution. Structural defects are responsible not only for part of the catalytic activity, but also for oxygen mobility within the solid's crystal lattice due to the non-stoichiometry created by the substitution. The presence of ionic vacancies affects catalytic activity by favouring (or not) reactant adsorption from the gas phase [7].

In this article, the effect of the partial substitution of calcium for lanthanum on the kinetics of methane combustion over $La_{1-x}Ca_xFeO_3$ perovskites is investigated.

EXPERIMENTAL

Preparation

$La_{1-x}Ca_xFeO_3$ (x=0.0, 0.2, 0.4) perovskites were prepared by the citrate method [8], with a 10% of excess over the number of ionic equivalents of cations. The resulting solution stirred at room temperature and evaporated under vacuum until gel formation. The gel dried in an oven up to 250°C and maintaining it overnight. The resulting powder crushed and sieved to obtain the required particle size (< 200 mm) and calcined at 700 °C in air for 6 h.

Characterization

Specific areas were calculated using the BET method from the nitrogen adsorption isotherms, recorded at the temperature of liquid nitrogen on a Micromeritics apparatus Model ASAP 2010. X-ray powder diffraction (XRD) patterns were obtained with nickel-filtered $CuKa_1$ radiation (l = 1.5418Å) using a Rigaku diffractometer controlled by a computer. Phase identification was carried out by comparison with the JCPDS-ICDD database cards. Temperature-programmed reduction (TPR) experiments were performed in a TPR/TPD 2900 Micromeritics system provided with a thermal conductivity detector. Reduction profiles were then recorded by passing a 5% H_2/Ar flow at a rate of 40 mL/min while heating at a rate of 10 °/min from ambient temperature to 900 °C. A cold-trap was placed just before the TCD of the instrument to remove the water from the exit stream. For the O_2-TPD experiments, the samples were exposed to oxygen for 1 h at 700° C, followed by cooling to room temperature in the same atmosphere. After switching the atmosphere to a helium flow, the sample was heated at a constant rate of 10°min^{-1} and the desorbed oxygen was monitored with a thermal conductivity detector.

Catalytic activity and kinetic studies.

The catalytic activity of the total combustion of methane was performed in a conventional flow reactor under atmospheric pressure. In each experiment, 0.3 g of catalysts (20-40 mesh) diluted with 1.5 g of SiC, of the same particle size, was loaded in a quartz reactor (i.d. 1.27 cm) with quartz fiber packed at the end of the catalyst bed. Gas flow rates were carefully adjusted by means of mass flow controllers (Brooks 5850E). Prior to each experiment, the catalyst was treated with 1000 mL min^{-1} (STP) of synthetic air for 1 h at 500°C, in order to eliminate probable carbonates and hydroxides formed at the surface. At this temperature, the oxidant gas was switched to the reactant gaseous mixture for 1 h. After that, the sample was cooled down to 300°C and stabilized for 30 min prior to the catalytic test. The thermocouple was placed inside the reactor just at the beginning of the catalysts bed. The inlet and outlet concentration of methane and carbon dioxide were analyzed using an on-line gas chromatograph Hewlett Packard model HP 4890D with thermal conductivity detector. The column used was a 3 meter capillary Supelco 25462, and helium was used as a carrier gas. The reproducibility of the results was verified by carrying out each test three times.

RESULTS AND DISCUSSION

Catalysts characterization

Table 1 summarizes the S_{BET} values. The lowest BET area (21 m^2g^{-1}) is found in the unsubstituted $LaFeO_3$ and partial substitution of lanthanum by calcium increase the value of BET area. X-ray diffraction patterns are shown in Figure 1. Pure $LaFeO_3$ corresponds to the orthorhombic (JC-PDF 371493) structure. As the Ca substitution increases, changes corresponding to lattice contraction are observed. Only CaO is detected as a segregated phase for x_{Ca}=0.4 at 2θ = 37.3°. Temperature-programmed reductions (TPR) are shown in Figure 2. No reduction of $LaFeO_3$ takes place and for x_{Ca}=0.2 a small peak indicative of a slight reduction degree increasing for x_{Ca}=0.4. The higher hydrogen consumption can be explained by the higher Fe^{4+} ions amount generated to compensate the charge unbalance. At higher temperatures, the hydrogen consumption increases linearly with temperature and no maximum could be detected up to 700°C. The O_2-TPD profiles are shown in Figure 3. Physisorbed species at low temperatures and the presence of a-oxygens as a shoulder for the pure $LaFeO_3$ perovskites, with an increase in intensity shifting towards higher temperatures as x_{Ca} values increase. The so-called β-oxygen, less present at 400°C for the pure $LaFeO_3$ show a noticeable increase in intensity upon the

e-mail: gpecchi@udec.cl

calcium substitution. Since this peak is associated with the lattice oxygen or with oxygen species occupying inner vacancies, the evolution of this oxygen species is a measurement of the replacement of La^{3+} for Ca^{2+} in the perovskite structure. The TPD–MS experiments confirm that the evolved gas and the He flow only contain oxygen. It is also observed, Figure 4, that a low substitution levels, $x < 0.1$, the amount of desorbed oxygen keeps nearly constant, indicating that the charge compensation comes almost entirely from the oxidation state increase of a part of the iron ions from Fe^{3+} to Fe^{4+}. At higher substitution levels, instead, the amount of desorbed oxygen becomes increasingly more important, suggesting that charge compensation comes mainly from the formation of oxygen vacancies even though the amount of Fe^{4+} also increases, however this increment is always lower than that necessary to charge balance.

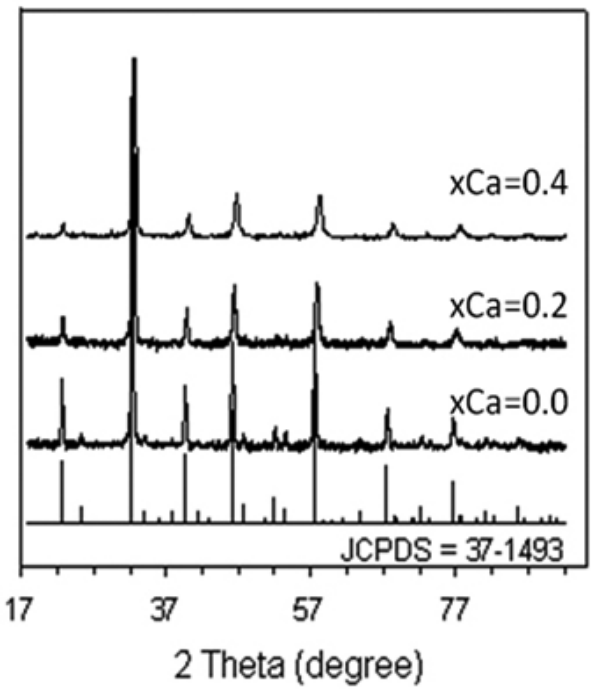

Figure 1. X-ray diffraction patterns.

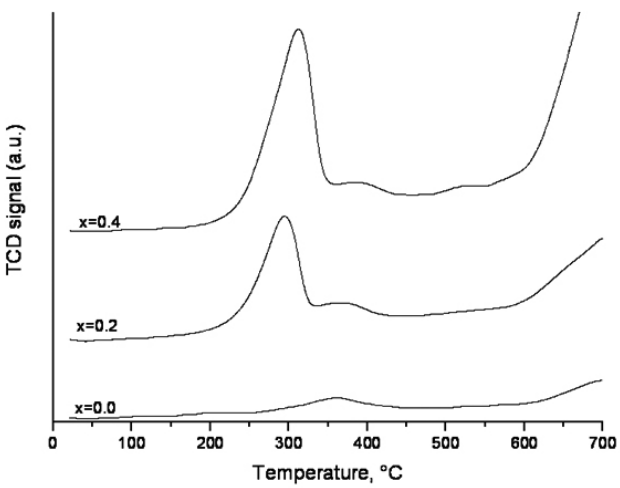

Figure 2. Temperature-programmed reduction.

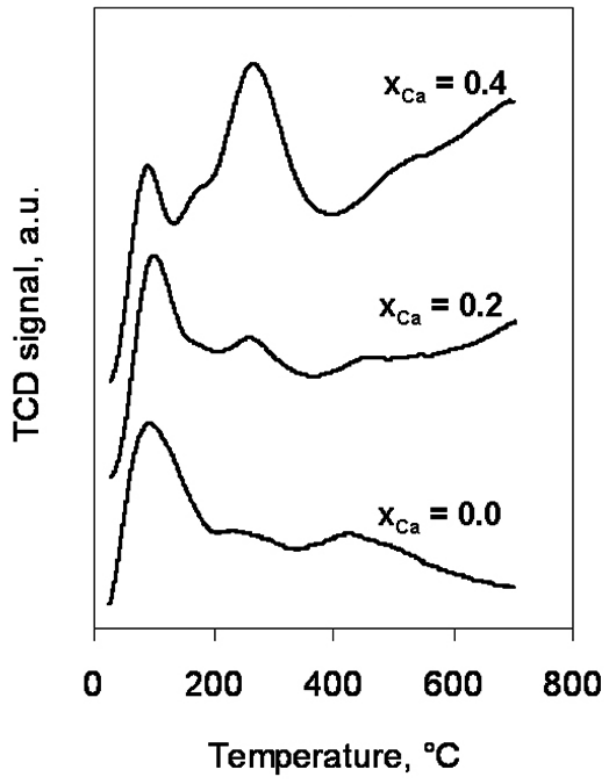

Figure 3. Oxygen-temperature programmed desorption profiles.

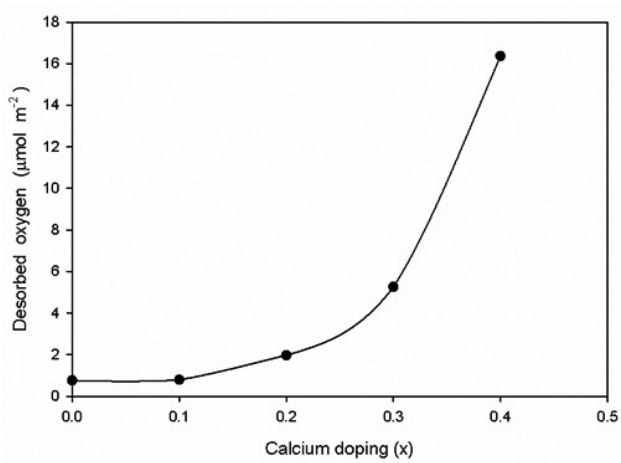

Figure 4. Desorbed oxygen vs calcium doping x.

Catalytic activity

The studied perovskite systems were tested in methane combustion using 37000 ppmv of methane, 23.22% of O_2, and He as balance in a flow reactor using a total flow of 300 $mLmin^{-1}$. The light-off curves are shown in Figure 5. The ignition temperature (T_{50}), defined as the temperature required to reach 50% conversion, decreases linearly as the calcium substitution level increases, as it is shown in Table 1. These catalytic results can be related with the characterization results as follows. The X-ray patterns of the substituted perovskites are monophasic and they show the same lines that $LaFeO_3$, although the line shift to higher 2θ angle values as the calcium doping level increases, Figure 6, is indicative of a lower interplanar distance and consequently, a decrease of the cell volume, as it can be seen in Figure 7.

The ionic radius of Ca^{2+} 12-coordinated (0.134 nm) is very similar to that of La^{3+} (0.136 nm), therefore the cell volume should be very slightly affected by this substitution. However, in order to preserve the electroneutrality upon

the substitution, an increase of the iron oxidation state from Fe^{3+} to Fe^{4+} must occur or oxygen vacancies must be generated, or both. The differences in the ionic radius of iron in different oxidation states explain the change in the cell volume, Fe^{3+} (0.0645 nm) and Fe^{4+} (0.0585 nm). In other words, the 2θ value shift and the decrease in the cell volume are direct effect of the existence of some iron in oxidation state (IV) and consequently confirm its presence. On the other hand, since both magnitudes show a linear dependence on the calcium substitution level we hypothesize that the amount of Fe^{4+} increases linearly with the calcium doping x.

Table 1. Specific BET area, oxygen desorption amount and ignition temperature for $La_{1-x}Ca_xFeO_3$ perovskites.

	x_{Ca}	S_{BET} m^2g^{-1}	O_2 des, $mmolg^{-1}$	$T_{50\%}$, °C
$LaFeO_3$	0.0	21	16	512
$La_{0.8}Ca_{0.2}FeO_3$	0.2	38	75	502
$La_{0.6}Ca_{0.4}FeO_3$	0.4	33	540	487

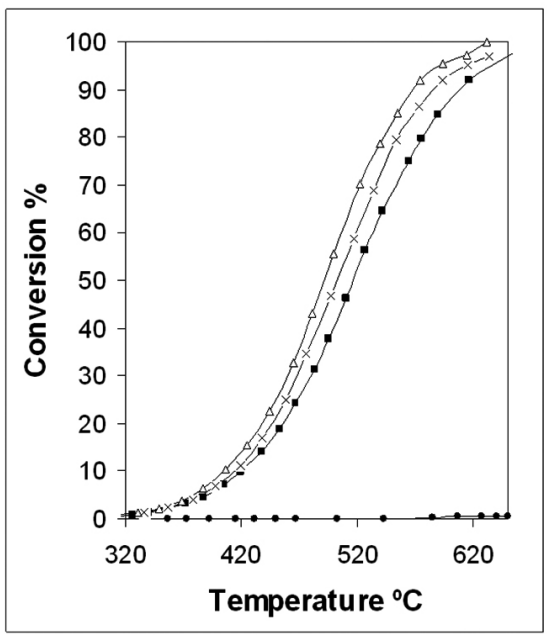

Figure 5. Light-off curves. (■) x_{Ca}=0.0; (´) x_{Ca}=0.2; (D) x_{Ca}=0.4; (o) non catalyzed.

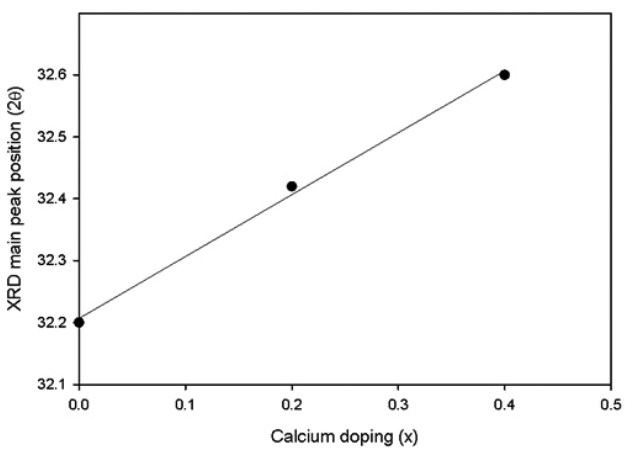

Figure 6. XRD main peak position (2θ) as a function of the calcium doping x.

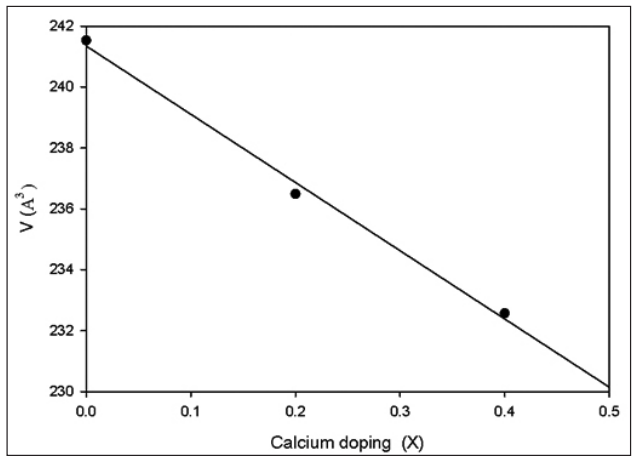

Figure 7. Unit cel volume vs. calcium doping x.

Kinetics studies

All catalysts were tested for methane oxidation activity by varying partial pressures of oxygen and methane. In each case, the only detected reaction products were carbon dioxide and water. The oxidation activity was evaluated using the initial rate method at the low methane conversion (< 20%) to ensure the absence of mass transfer limitations at the reaction conditions. At low temperatures, like those considered in this study, the oxidation rate depends on both P_{CH4} and P_{O2}. Therefore, the results can be expressed by the empirical rate equation:

$$r = k\, P_{CH_4}^{m}\, P_{O_2}^{n} \qquad (1)$$

where r is the oxidation rate, m and n are the partial reaction orders for methane and oxygen, respectively.

At oxygen partial pressure constant this equation takes the form:

$$\ln r = \ln k^{*} + m \ln P_{CH_4} \qquad (2)$$

where:

$$\ln k^{*} = \ln k + n \ln P_{O_2} \qquad (3)$$

Therefore, the plot of ln r vs ln P_{CH4} should be a straight line with slope equals to m, the order respect to methane, as shown in Figure 8. This figure shows a series of nearly parallel lines whose intercept depend on the oxygen partial pressure. Thus, the plot of the intercept as function of ln P_{O2} should be also a straight line with slope equals to n, the order respect to oxygen, and the constant coefficient equals to ln k, Figure 9. Therefore, the linear regression analysis of eqns. (2) and (3) allows to obtain the values of m, n and k . These results are shown in Table 2. The reaction order for methane is consistently 0.8 (ca. 1.0), while the reaction order for oxygen varies with temperature and the level of Ca-doping. It can be observed a slight inverse dependence on temperature, however this decrease is within the experimental error. Whereas, a more strong dependence on the level of calcium doping is observed, going from 0.5 to about 0.3 for x= 0.0 and x= 0.4, respectively. This finding suggests the participation of lattice oxygen at the catalyst surface, as it is discussed below.

The apparent activation energies were determined by Arrhenius plots of ln k vs 1/T in each case, Figure 10. The values of the apparent activation energy and pre-exponential factor A are compiled in Table 2. The doped perovskites show lower activation energies, which in turn explain their higher catalytic activity. It is observed, also, that the value of the activation energy is not affected by the level of Ca-doping. This finding seems to support the hypothesis regarding the higher reaction rate is due to an increase in the number of active sites rather than an increase in the activity of the separate sites, which in turn it is reflected in a larger pre-exponential factor as shown in Table 2. The higher the Ca content the higher the number of active sites, whose effectiveness does not seem to be affected, in first approximation, by the presence of a higher number of neighboring active sites, as proposed by Saracco et al. [9].

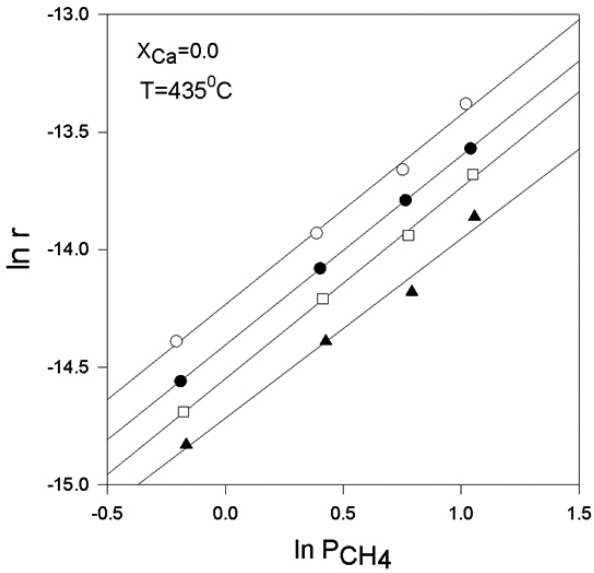

Figure 8. ln r as a function of ln P_{CH4}. Partial pressure of O_2 Open circle: 23.5 kPa; solid circle: 18.0 kPa, square:13.0 kPa; triangle 8.0 kPa.

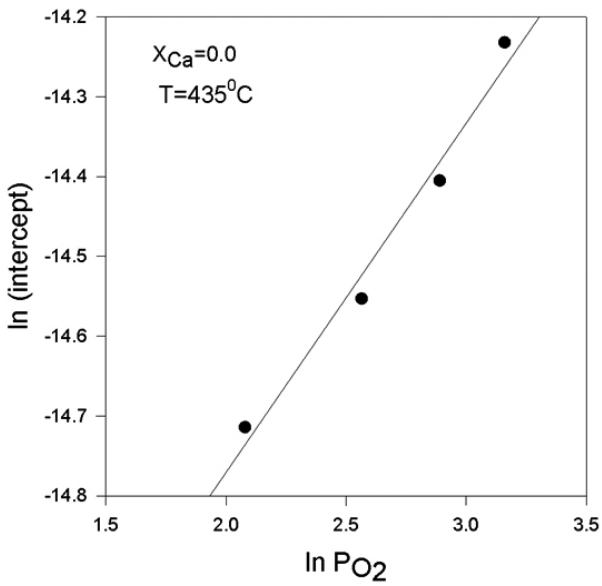

Figure 9. Neperian logarithm of the intercept as a function of ln P_{O2}

The effect of the variation of the methane partial pressure at a constant oxygen partial pressure on the rate of reaction of methane oxidation is shown in Figure 8. It is observed that the reaction rate is a function nearly linear on the methane partial pressure; actually its order is 0.8 as determined above. On the other hand, the dependence of the reaction rate on the oxygen partial pressure is shown in Figure 11 for $LaFeO_3$. These findings seem to support the hypothesis that the reaction follows an Rideal-Elay type mechanism, as it has been reported for the catalytic combustion of methane over perovskites, including $LaFeO_3$ [5,9,10]. The combustion involves reversibly chemisorbed oxygen atoms which are continuously supplied from the gas phase and surface oxygen originating from the lattice.

Thus, the reaction rate may be expressed as [10]:

$$r = k_1 P_{CH_4} + k_2 P_{O_2}^{1/2} P_{CH_4} \qquad (4)$$

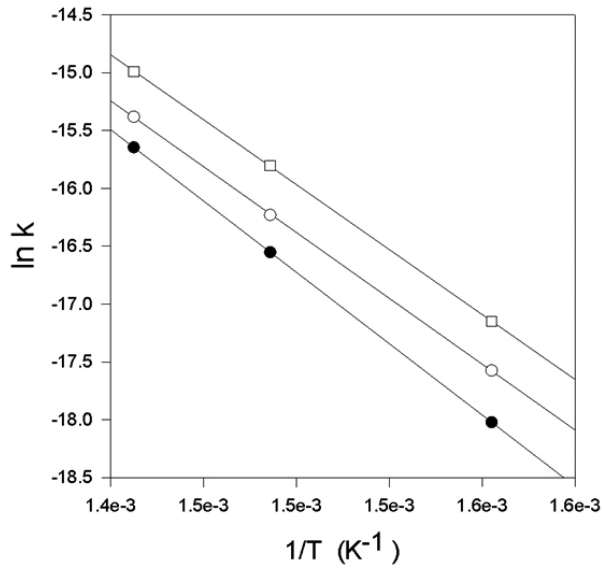

Figure 10. Arrhenius plot for x_{Ca}=0.0 Solid circle: 350°C; Open circle: 400°C; square: 435°C.

Table 2. Kinetic results in the combustion of methane over $La_{1-x}Ca_xFeO_3$ perovskites.

Catalyst	Temp °C	m	n	k x 10^{12} molg^{-1}s^{-1}Pa$^{-1.5}$	E_a kJmol^{-1}	A x10^4 molg^{-1}s^{-1}Pa$^{-1.5}$
$LaFeO_3$	350	0.8	0.5	0.44	105.7	3.2
	400	0.8	0.5	2.00		
	435	0.8	0.5	5.10		
$La_{0.8}Ca_{0.2}FeO_3$	350	0.8	0.4	0.72	95.5	0.73
	400	0.8	0.4	2.80		
	435	0.8	0.4	6.60		
$La_{0.6}Ca_{0.4}FeO_3$	350	0.8	0.3	1.10	94.6	0.94
	400	0.8	0.3	4.40		
	435	0.8	0.3	9.80		

where k_1 is the rate constant for reaction with surface oxygen associated with the substrate lattice, and k_2 is the rate constant for reaction with chemisorbed oxygen. The contribution of each of these two oxygen sources to methane combustion at a specified temperature can be derived from a plot of the rate against the square root of oxygen partial pressure. The intercept represents the contribution of lattice oxygen to the reaction rate. The gas-phase oxygen contribution is proportional to the slope of the line. Thus, from the intercept and slope it is possible to evaluate k_1 and k_2. From Figure 11 it is possible to observe the null intercept for the three temperatures considered in this study, indicating that the contribution of lattice oxygen is quite negligible for $LaFeO_3$.

On the other hand, for x = 0.4 is observed that the intercept clearly differs from zero, Figure 12, indicating the increasing participation of lattice oxygen in the combustion kinetics of methane as the calcium doping goes up, as consequence of the oxygen vacancy formation. This finding suggests that other effect of calcium is to turn the lattice oxygen into reactive species at relatively low temperatures. The substitution of lanthanum by a lower valence cation, as calcium, entails both the formation of oxygen vacancies and oxidation of some iron ions from Fe^{3+} to Fe^{4+}, in order to preserve the electroneutrality. The global process can be represented by the following defect reactions:

Oxygen vacancy formation by substitution of Ca for La in the lattice:

$$2CaO + 2La_{La} + O_O^x \rightarrow 2Ca'_{La} + V_O^{\bullet\bullet} + La_2O_3$$

Hole formation by equilibrium between gaseous oxygen and oxygen vacancy:

$$V_O^{\bullet\bullet} + \frac{1}{2}O_2 \leftrightarrow \quad O_O^x + 2h^\bullet$$

Fe^{4+} formation by oxidation of Fe^{3+}:

$$Fe\ {}^{x}_{Fe} + h^\bullet \leftrightarrow \quad Fe\ {}^{\bullet}_{Fe}$$

Such a condition promotes an important increase in the reactivity of the lattice oxygen close to the Fe^{4+} ions. The values of the constants k_1 and k_2 are compiled in Table 3. The respective Arrhenius plots of the two rate constants over a range of temperature allow to obtain the activation energies, E_1 and E_2, for each of the two processes, Figure 13 and Table 3. From this table it is possible to observe a remarkable decrease in the activation energy for the lattice oxygen, denoting the key role of calcium doping in turning the lattice oxygen into more reactive species as the level of doping increases. The values of k_1 and k_2 so obtained are validated recalculating the rate of combustion of methane using eqn. (4) and plotting the calculated rate vs. the experimental rate, Figures 14 and 15. In all the cases the experimental rate is reproduced pretty well. The squared correlation coefficients for the two cases shown are 0.99, confirming the reliability of the values of k_1 and k_2 calculated in this study.

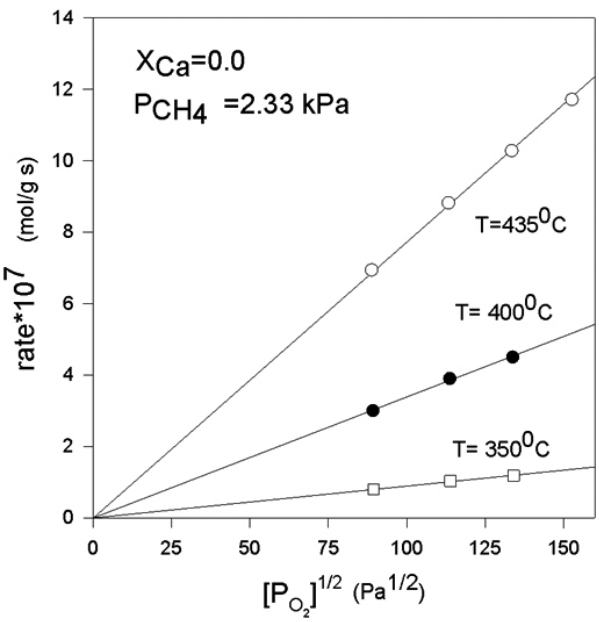

Figure 11. Reaction rate as a function of $(P_{O2})^{1/2}$ for x_{Ca}=0.0

Table 3. Kinetic parameters according the mechanism of Rideal-Elay for the combustion of methane over $La_{1-x}Ca_xFeO_3$ perovskites.

Catalyst	Temp °C	k_1 x10^{11} molg^{-1}s^{-1}Pa$^{-1.5}$	k_2 x10^{12} molg^{-1}s^{-1}Pa$^{-1.5}$	E_1 kJmol^{-1}	E_2 kJmol^{-1}
$LaFeO_3$	350	---	0.38	---	93.0
	400	---	1.40		
	435	---	3.30		
$La_{0.8}Ca_{0.2}FeO_3$	350	0.89	0.40	120.7	75.5
	400	4.30	0.93		
	435	15.0	2.40		
$La_{0.6}Ca_{0.4}FeO_3$	350	3.80	0.21	73.1	114.1
	400	9.90	1.20		
	435	21.0	2.90		

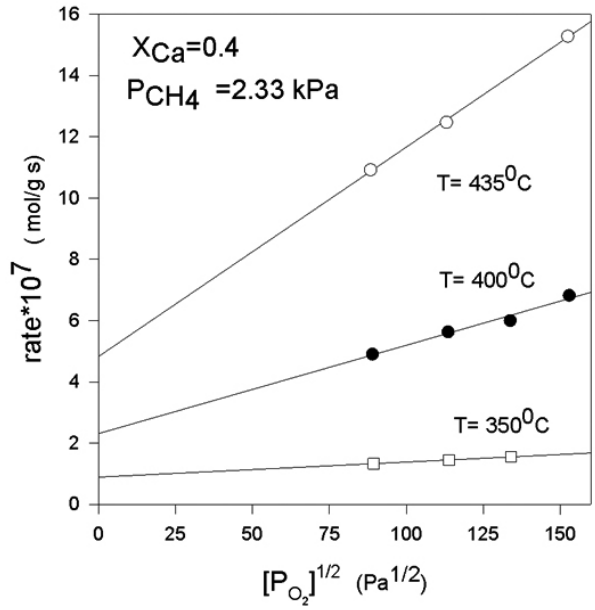

Figure 12. Reaction rate as a function of $(P_{O2})^{1/2}$ for x_{Ca}=0.4

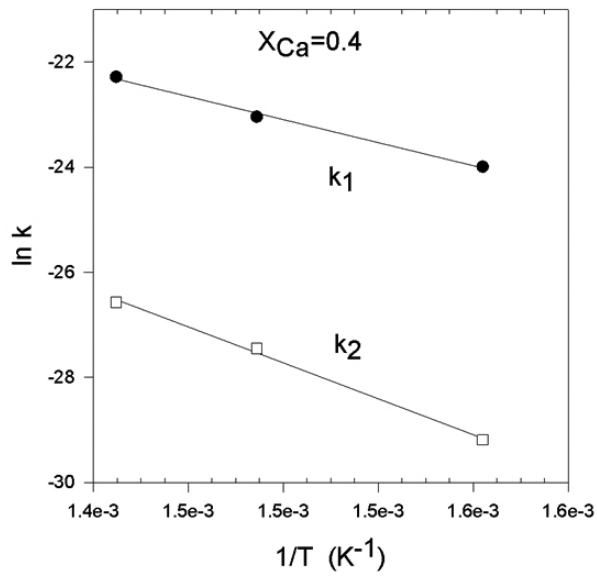

Figure 13. Arrhenius plot for x_{Ca}=0.4.

CONCLUSIONS

In this article the reaction kinetics of methane combustion over $La_{1-x}Ca_xFeO_3$ perovskites, x_{Ca} = 0.0, 0.2 and 0.4 was studied. The results show that the catalytic activity for the combustion of methane is higher in the calcium-doped perovskites. It is found that this higher catalytic activity is related to a lower activation energy. The value of the activation energy is not affected by the level of Ca-doping. The observed difference in the catalytic activity between the doped perovskites is interpreted as a consequence of the so-called compensatory effect, i.e., a larger pre-exponential factor which result from the higher number of active sites promoted by defect reactions triggered by the substitution of lanthanum by calcium. The defect reactions involve the formation of iron ions in the unusual oxidation state (IV) and oxygen vacancies. The presence of Fe^{4+} ions explain the compensatory effect, i.e., the differences in the pre-exponential factor, therefore the actives sites may be directly related to this unusual oxidation state of iron. On the other hand, the oxygen vacancies account for the increasing participation of lattice oxygen in the combustion

kinetics as the calcium doping increases. The experimental results were satisfactorily fitted to the Rideal-Elay mechanism.

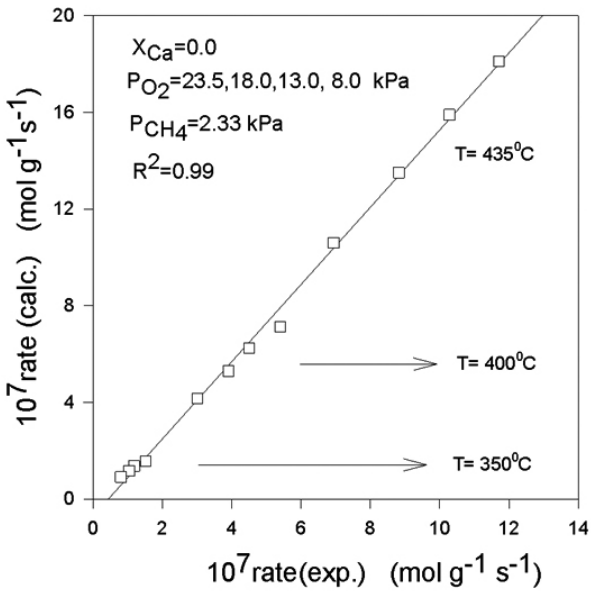

Figure 14. Calculated rate versus experimental rate for x_{Ca}=0.0

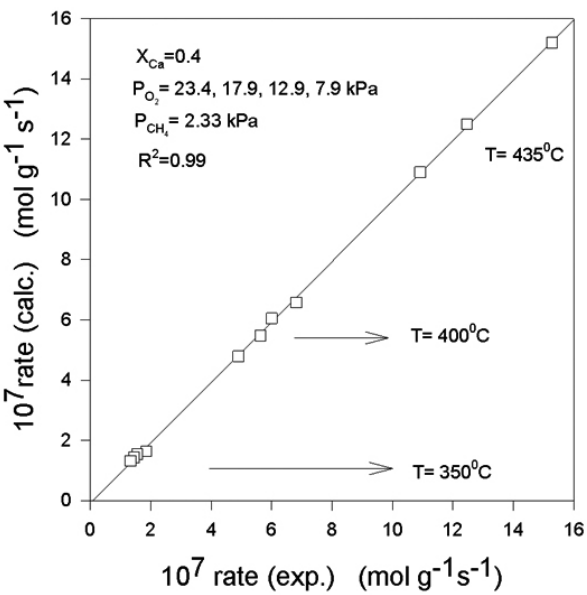

Figure 15. Calculated rate versus experimental rate for x_{Ca}=0.4

ACKNOWLEDGMENTS

The authors thank CONICYT, FONDECYT Grant 1090018

REFERENCES

1. Ferri D, Forni L *Appl Catal B: Environmental* **16**, 119, (1988)
2. Yu Z, Gao L, Yuan S, Wu Y, *J Chem Soc Faraday Trans,* **88**, 3245 (1992).
3. Marchetti L, Forni L, *Appl Catal B: Environmental,* **15**, 179 (1998).
4. Popescu I, Urda A, Yuzhakova T, Marcu IC, Kowacs J, Sandulescu I, *C R Chimie,* **12**, 1072 (2009).
5. McCarty JG, Wise H, *Catalysis Today,* **8**, 231 (1990).
6. Gelling PJ, Bouwmeester HJM, *Catalysis Today,* **58**, 1 (2000).
7. Merkle R, Maier J, *Topics in Catalysis,* **38**, 141 (2006).
8. Courty P, Ajot H, Marcilly C, Delmon B, *Power Technol,* **7**, 21 (1973).
9. Saracco G; Scibilia G, Iannibello A, Baldi G, *Appl Catal B: Environmental,* **8**, 229 (1996).
10. Arai H, Yamada T, Eguchi K, Seiyama T*, Appl Catal,* **26**, 265 (1986).